JOURNAL OF Materials CHEMISTRY

The insulator–metal transition upon lithium deintercalation from $LiCoO_2$: electronic properties and ^7Li NMR study

Michel Ménétrier, Ismael Saadoune, Stéphane Levasseur and Claude Delmas*

Institut de Chimie de la Matière Condensée de Bordeaux-CNRS and Ecole Nationale, Supérieure de Chimie et Physique de Bordeaux, Château de Brivazac, Av. Dr A. Schweitzer, 33608 Pessac cedex, France. E-mail: delmas@icmcb.u-bordeaux.fr

Received 4th January 1999, Accepted 1st March 1999

Samples of $Li_xCoO_2 (0.5 \leqslant x \leqslant 1)$ have been prepared by electrochemical deintercalation from high temperature $LiCoO_2$ and are characterized by X-ray diffraction, electrical measurements and ^7Li MAS NMR spectroscopy. X-Ray diffraction studies as a function of x are in good agreement with literature data and suggest that the two-phase domain for $0.75 \leqslant x \leqslant 0.94$ is not due to structural reasons. Electrical conductivity and thermoelectronic power measurements evidence a gradual change in the electronic properties from localised to delocalised electrons upon lithium deintercalation. ^7Li MAS NMR suggests that the metal–non metal transition is the driving force for the existence of the biphasic domain.

Introduction

$LiCoO_2$ has been used as a positive electrode material in commercial Li–ion batteries for over ten years, with an extremely fast growth of the market. In 1980, Goodenough and coworkers[1] demonstrated the ability of $LiCoO_2$ to reversibly deintercalate lithium. $LiCoO_2$ crystallizes in the rhombohedral system (space group $R\bar{3}m$) with the layered α-$NaFeO_2$ type structure. The structure can be thought of as an ordered rocksalt type with an ABCABC stacking of the oxygen planes and the Co and Li ions ordered in alternate octahedral sites of (111) planes.

The phase changes upon deintercalation have been extensively studied, for they are believed to influence the reversibility of the intercalation/deintercalation process.[2–4] Reimers and Dahn[2] reported, in a detailed *in situ* X-ray study, the existence of a two-phase region corresponding to a voltage plateau for $0.75 \leqslant x \leqslant 0.93$ and the presence of a monoclinic distortion for $x = 0.5$ attributed to an interslab lithium/vacancy ordering. The two phases with $x = 0.93$ and 0.75 both crystallize in the rhombohedral system with only a small variation in the cell parameters; this suggests that the origin for the biphasic phenomenon is not structural.

Only a few papers describe the physical properties of this material, the conclusions of which are briefly outlined hereafter. Studies carried out on Li_xCoO_2 crystallised thin films with microarray electrodes showed that the electronic conductivity increases considerably with lithium deintercalation $(0.9 \leqslant x \leqslant 1.0)$. Furthermore, they showed that the metallic behavior of Li_xCoO_2 induced by the first Li extraction does not revert to its original insulating state in the following redox cycles.[5,6] Honders *et al.*[7] indicated that the electrical transport takes place through moving electron holes in a Co^{III} valence band and suggested the existence of a few Co^{IV} in the starting oxide lattice due to a small departure from stoichiometry. Moreover, they showed a strong decrease in the absolute value of the Seebeck coefficient related to an increase in the conductivity upon deintercalation. Electronic conductivity measurements were performed by Molenda *et al.*[8] who showed a very strong increase in conductivity upon deintercalation. They observed a semiconductor behavior for the lithium-rich phases and a metallic one for the more deintercalated ones. Their thermoelectronic power measurements agree globally with those by Honders *et al.*[7] for the most deintercalated phases, but are significantly different for compositions close to $LiCoO_2$. Moreover, Molenda *et al.*[8] explained their results under the hypothesis of trivalent and tetravalent cobalt in the high spin configuration, which is quite unexpected in such layered phases. Several studies (magnetic and electric properties) performed in our laboratory, both for $LiNi_yCo_{1-y}O_2$ $(0.1 \leqslant y \leqslant 0.9)$ solid solutions and for cobalt substituted nickel oxyhydroxides showed that cobalt ions are in a low spin trivalent state due to the strong stabilization of the t_2^6 configuration.[9,10] The low spin configuration of trivalent cobalt is also consistent with the short Co–O distance (1.92 Å) found in the Rietveld refinement analysis of the $LiCoO_2$ neutron diffraction pattern.[11]

^7Li NMR is very sensitive to the presence of electron spins or delocalised electrons, and can thereby lead to a very precise characterisation of the local structure in intercalation compounds. In particular, it unambiguously confirms that Co^{III} ions are in the low spin state in $LiCoO_2$.[12–14] To our knowledge, the only NMR study reported so far for deintercalated Li_xCoO_2 phases is that by Greenbaum and coworkers.[15] In that paper, the width of the static ^7Li NMR line was interpreted in terms of localised electron spins in the whole range of compositions studied $(0.4 \leqslant x < 1)$. The MAS spectrum for $x = 0.9$, which exhibited two signals, was interpreted as indicating two magnetically inequivalent sites in this material, with no reference being made to the two-phase domain for this composition range.

In the context of our general studies on Li_xMO_2 layered oxides and more specifically for a better understanding of the processes involved in initial lithium deintercalation, we have performed a detailed study of the Li_xCoO_2 system for $0.5 \leqslant x \leqslant 1$ by X-ray diffraction, electrical measurements and ^7Li MAS NMR.[16] Very recently, a theoretical study of the Li_xCoO_2 phase diagram was carried out by Van der Ven *et al.*,[17] using first principles total energy calculations within the local density approximation; this study did not predict the two-phase region found experimentally for $0.75 \leqslant x \leqslant 0.94$. The authors concluded that the two-phase domain must be due to an insulator to metal transition, since their calculations did not explicitly take electron correlations into account and could therefore not predict the relative stability of otherwise similar metallic and non-metallic phases.[17]

Experimental

The $LiCoO_2$ starting material was prepared by calcination of a pelletized stoichiometric mixture of Li_2CO_3 (Rhône Poulenc

Rectapur, 99% min.) and Co_3O_4 [calcination at 450 °C for 12 h under O_2 of $Co(NO_3)_2{\cdot}6H_2O$ Carlo Erba 99% min.) at 600 °C for 12 h under dry O_2, followed by two successive heat treatments at 900 °C for 24 and 12 h with intermediate grinding.

Electrochemical studies were carried out with Li|$LiClO_4$–ethylene carbonate (EC)–dimethyl carbonate-(DMC)|Li_xCoO_2 cells. For classical electrochemical experiments, the positive electrode consisted of a mixture of 90 wt% active material and 10% carbon black. For the electrochemical preparation of partially deintercalated phases for electrical measurements and ^{7}Li MAS NMR, sintered pellets (8 mm in diameter) of the starting material were used as positive electrode (600 MPa pressure and thermal treatment at 800 °C for 12 h under oxygen). The cells assembled in an argon-filled dry box were charged at 100 μA cm^{-2} (m_{LiCoO_2} = 180 mg). For the thermodynamic potential measurements (open circuit voltage), the charge process was interrupted by relaxation periods until the slope of the voltage–time curve was <0.1 mV h^{-1}.

The X-ray diffraction patterns were recorded *ex situ* using an INEL CPS 120 curve position sensitive detector with a cobalt anode or a Philips PW1820 powder diffractometer with Cu-Kα radiation.

Electronic conductivity measurements were carried out with the four probe direct current method in the temperature range 100–300 K. The thermoelectronic power measurements were performed with a homemade equipment.[18]

^{7}Li MAS NMR spectra were recorded on a Bruker MSL 200 spectrometer at 77.7 MHz, with a standard Bruker MAS probe. The samples were mixed with dry silica (typically 50 wt%, depending on the amount of material available), in order to facilitate the spinning and improve the field homogeneity, since they may exhibit metallic or paramagnetic properties. The mixture was placed in 4 mm diameter zirconia rotors in a dry box. No change in the NMR signal was observed even for rotors kept several days out of the dry box, indicating a satisfactory air-tightness. A synchronised echo pulse sequence was utilised, in order to facilitate the phasing of all the spinning sidebands, and to ensure the observation of possibly very wide signals. The 90° pulse duration was 3.5 μs, the spinning speed was in the range 10–12 kHz, and the interpulse delay was varied accordingly (100–83.3 μs). The spectral width was in the range 100–500 kHz. The recycle time was 10 s, which avoids the possible saturation of signals with no hyperfine interaction, with 600–2000 scans per spectrum. The external reference was a 1M LiCl aqueous solution.

Results and discussion

The X-ray diffraction pattern of the starting material is characteristic of the layered HT-$LiCoO_2$ structure. This material crystallises in the rhombohedral system (space group $R\bar{3}m$). The refined hexagonal cell parameters [a_{hex} = 2.8155(2) and c_{hex} = 14.049(5) Å] are in very good agreement with those reported in the literature.[1–3,11]

X-Ray diffraction study

In order to follow the change in the crystal structure of $LiCoO_2$ during electrochemical deintercalation, XRD patterns of Li_xCoO_2 samples for $0.7 \leqslant x \leqslant 1.0$ were recorded. Fig. 1 shows the diffraction patterns of some Li_xCoO_2 samples. All materials exhibit narrow diffraction lines, showing that the crystallinity of the starting material is maintained during deintercalation. The XRD patterns were indexed in the hexagonal system. A closer examination of the (003) line evolution during deintercalation is shown in Fig. 2. The $0.94 < x \leqslant 1.0$ domain appears to be a solid solution, while the gradual disappearance of the original peak at 4.67 Å ($2\theta = 18.98°$) and the appearance of a new peak at lower angle ($2\theta = 18.80°$)

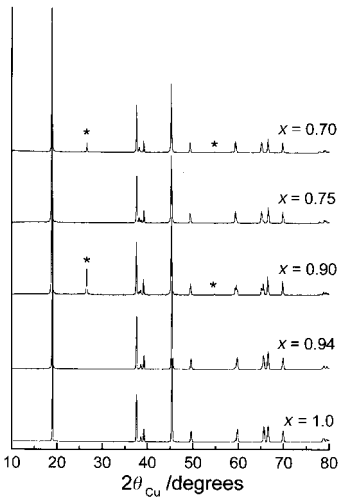

Fig. 1 X-Ray diffraction patterns of the electrochemically deintercalated Li_xCoO_2 samples (* = carbon).

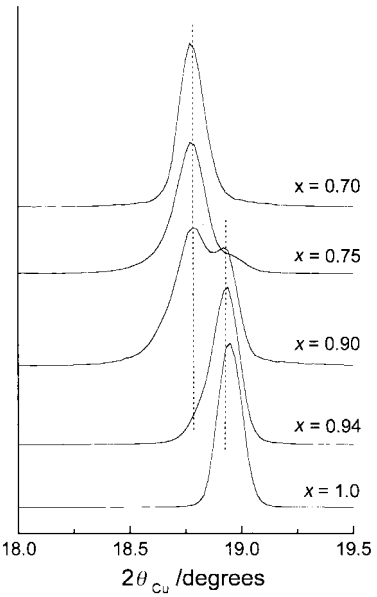

Fig. 2 Expansion of the (003) Bragg reflection of the electrochemically deintercalated Li_xCoO_2 samples.

during further lithium extraction clearly indicate the existence of a two-phase domain for $0.75 \leqslant x \leqslant 0.94$. It should be noted that $Li_{0.94}CoO_2$ and $Li_{0.75}CoO_2$ compositions are biphasic but the very small quantity of the minor phase in both cases confirms that these compositions are very close to the extreme limits of the two-phase domain. All these results are in very good agreement with the *in situ* X-ray study by Reimers and Dahn.[2] The evolution of the cell parameters during deintercalation is shown in Table 1. The general trend corresponds to that generally observed in layered oxides upon deintercalation: an increase in the *c* parameter due to the weakening of the

Table 1 Hexagonal cell parameters for Li_xCoO_2 samples

x in Li_xCoO_2	a/Å	c/Å	c/a
1.00	2.8155(2)	14.049(5)	4.99
0.98	2.815(3)	14.051(2)	4.99
0.94[a]	2.813(1)[a]	14.056(9)[a]	4.99[a]
0.75[a]	2.810(1)[a]	14.193(4)[a]	5.05[a]
0.70	2.811(1)	14.196(2)	5.05
0.60	2.810(1)	14.287(6)	5.08

[a]Limit of the solid solution; contains traces of the other phase.

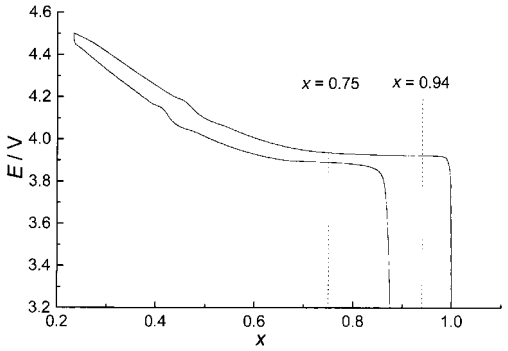

Fig. 3 First galvanostatic charge–discharge cycle of an Li||Li_xCoO_2 electrochemical cell ($J=100$ μA cm^{-2}; $m_{LiCoO_2}=30$ mg).

interslab cohesion and a decrease in the *a* parameter resulting from cobalt oxidation, and confirms that the parameters for the two limit phases, $Li_{0.94}CoO_2$ and $Li_{0.75}CoO_2$, are fairly close. Moreover, these two phases are hexagonal. In the homologous Li_xNiO_2 system, the first order transitions observed are related to changes in crystal symmetry induced by lithium/vacancy ordering.[19,20] In the Li_xCoO_2 system, a lithium/vacancy ordering with a rhombohedral symmetry could be thought of for the $Li_{0.75}CoO_2$ composition. Nevertheless, the presence of a large solid solution region for $0.50\leqslant x\leqslant 0.74$ makes it unlikely that, in such a phase diagram where only rhombohedral phases are involved, the driving force for the first order transition be lithium/vacancy ordering. This is indeed confirmed by the theoretical calculations by Van der Ven *et al.*[17]

Electrochemical study

Fig. 3 shows the first galvanostatic charge and discharge curves of an Li||Li_xCoO_2 cell at low rate ($J=100$ μA cm^{-2}, $m_{LiCoO_2}=30$ mg). The shift in x observed for the discharge curve with respect to the charge one partly results from the decomposition of the electrolyte at high potential. The cycling curve exhibits the particular feature expected for $x=0.5$.[2,3] For $0.75\leqslant x\leqslant 0.94$, a voltage plateau at *ca.* 3.93 V resulting from the existence of a two-phase domain confirms the X-ray results. The open-circuit voltage curve of the first steps of the charge process shown in Fig. 4 clearly evidences the narrow solid solution domain for $0.94<x\leqslant 1$ and the beginning of the biphasic region for $x=0.94$.

Electronic properties

Electronic conductivity. Fig. 5 shows the variation *versus* reciprocal temperature of the electronic conductivity of Li_xCoO_2 samples for x ranging from 1.0 to 0.55. Two different regimes are evidenced.

For those materials belonging to the lithium-rich solid solution, the electronic conductivity is thermally activated. The activation energy decreases rapidly when lithium is deintercalated. In all cases, the thermal variation does not strictly obey an Arrhenius law: the activation energy varies slightly with temperature (Table 2). It should be noted that the $Li_{0.94}CoO_2$ composition contains actually a very small amount of the lithium-rich end member of the lithium-poor solid solution, which may affect the observed conductivity values.

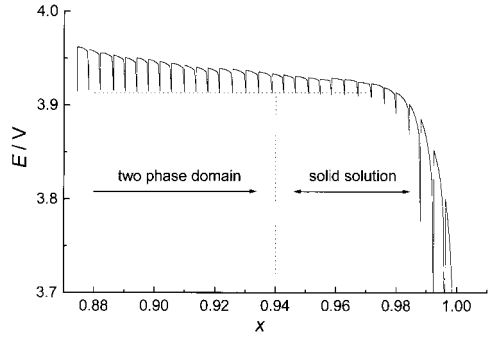

Fig. 4 Open circuit voltage curve of an Li||Li_xCoO_2 electrochemical cell ($J=100$ μA cm^{-2}; end of relaxation criterion: $\Delta V/\Delta t=0.1$ mV h^{-1}).

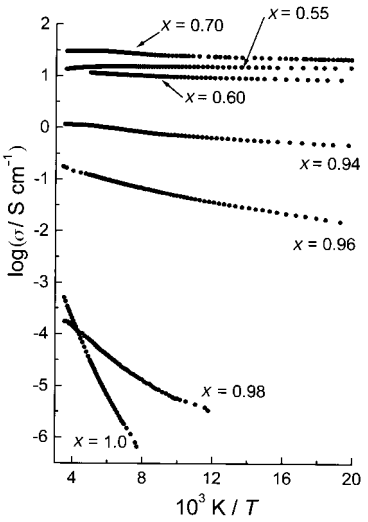

Fig. 5 Variation of the logarithm of the electrical conductivity *vs.* reciprocal temperature of the Li_xCoO_2 samples.

For Li_xCoO_2 phases with $0.50\leqslant x\leqslant 0.74$, the curves are almost flat, which indicates a metallic or a pseudometallic character. It can be seen that the conductivity values do not vary monotonously with the degree of deintercalation. It is well known that the absolute value of the conductivity on sintered pellets is very sensitive to their compactness. Moreover, for electrochemically deintercalated materials, the change in the unit cell volume leads to constraints and local loss of internal contacts which further alter the conductivity values. Nevertheless, the general shape of the curves unambiguously shows the electronic delocalisation. For the $Li_{0.55}CoO_2$ and $Li_{0.70}CoO_2$ samples, the variation of σ *versus* T is given in Fig. 6. For both phases, the increase in conductivity with decrease in temperature evidences a true metallic behavior between 175 and 300 K, while a more complicated behavior is observed at lower temperature.

Thermoelectronic power. Thermoelectronic power measurements for various Li_xCoO_2 compositions have been obtained in the temperature range 100–300 K and results are summarized in Fig. 7. The positive values of the Seebeck coefficient in the whole deintercalation range clearly establish that electron holes are the prevailing charge carriers. The high values of the thermoelectronic power of $Li_{0.98}CoO_2$ are typical of a semiconductor behavior, in good agreement with the results obtained by the electronic conductivity measurements. For the $Li_{0.94}CoO_2$ composition, which in addition contains traces of the metallic phase, the lower values of the Seebeck coefficient result from an increase in the number of charge carriers as

Table 2 Activation energy *vs.* the lithium amount x in the Li_xCoO_2 phases in different temperature ranges

x in Li_xCoO_2	1	0.98	0.96
ΔE_a/eV (190–290 K)	0.16	0.05	0.02
ΔE_a/eV (125–170 K)	0.11	0.04	0.01
ΔE_a/eV (80–100 K)	—[a]	0.02	0.01

[a]No data available.

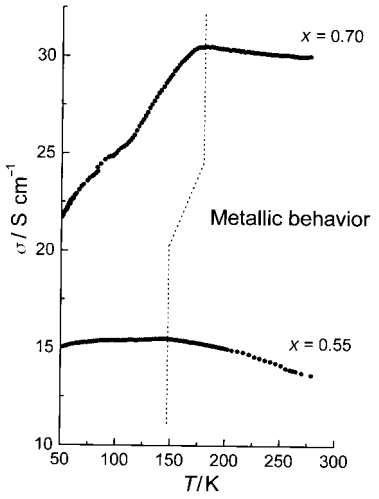

Fig. 6 Variation of the electrical conductivity *vs.* temperature for $Li_{0.70}CoO_2$ and $Li_{0.55}CoO_2$ phases.

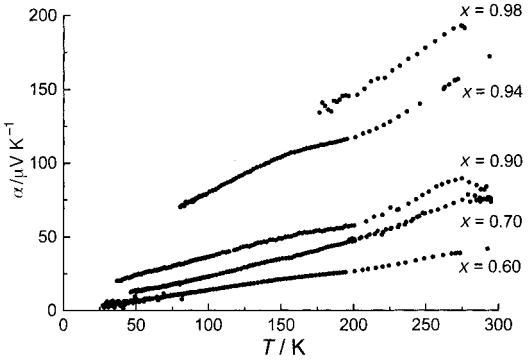

Fig. 7 Thermal variation of the Seebeck coefficient of the Li_xCoO_2 samples.

oxidation of the diamagnetic Co^{III} ions to paramagnetic Co^{IV} ions proceeds. Nevertheless, for both materials, the temperature dependence reflects a complex behavior. Finally, for the most deintercalated phases ($x \leqslant 0.70$), the quasi-linearity of the $\alpha = f(T)$ plots and the low values of the Seebeck coefficient, which tends to zero when temperature decreases, are typical of metallic behavior. For the $Li_{0.9}CoO_2$ composition which corresponds to the two-phase domain, an intermediate behavior is clearly observed.

Discussion. The electronic conductivity and the thermoelectronic power data clearly show the very different behavior of the lithium-rich and -poor materials.

In these materials, Co^{III} and Co^{IV} ions are in a low spin configuration, so that Co^{III} ions are diamagnetic ($t_2{}^6e^0$) and should not give rise to conduction. Therefore, the semiconductor type properties of starting $LiCoO_2$ suggest the presence of a few charge carriers in this material which can result from a small departure from stoichiometry. Lithium deintercalation, which increases the number of tetravalent ions, tends to decrease the activation energy; simultaneously, the conductivity is increased by several orders of magnitude.

The behavior of these semiconducting materials is quite different from that observed in the $Li_xNi_{0.8}Co_{0.2}O_2$ solid solution.[9] In the latter system, both electronic conductivity and thermoelectronic power measurements clearly show a small-polaron type conductivity ($\Delta E = 0.40$ eV, no thermal activation of the number of charge carriers). By contrast, the very low activation energy and the thermal variation of the Seebeck coefficient in the Li_xCoO_2 system are very similar to those previously reported by us for the $Li_xNi_{0.1}Co_{0.9}O_2$ solid solution.[14] In both systems, a continuous evolution from localised to delocalised states seems to be evidenced. Nevertheless, in the pure cobalt system, a two-phase mixture is observed for $0.75 \leqslant x \leqslant 0.94$ while in the mixed (Ni, Co) system, a solid solution was observed during lithium deintercalation.

In this type of layered structure, the presence of edge sharing octahedra leads to a direct t_{2g}–t_{2g} orbital overlap. As discussed by Goodenough,[21] in transition metal oxides, an electronic delocalisation through overlapping t_{2g} orbitals is expected if the bands are not completely filled and if the metal–metal distance is smaller than an empirical value R_c which, for 3d elements, can be calculated using eqn. (1):

$$R_{c(3d)} = 3.20 - 0.05m - 0.03(Z - Z_{Ti}) - 0.04S(S+1) \quad (1)$$

where m is the valence of M^{m+}, Z is the atomic number of M, Z_{Ti} is the atomic number of titanium and S is the effective spin of M.

In Li_xCoO_2 compounds, whatever the lithium amount, the Co–Co distance is smaller than the R_c value, as shown in Table 3, and, therefore, an electronic delocalisation is expected. In the lithium-rich solid solution, the proportion of Co^{IV} is very small so that the number of holes in the t_{2g} band is too small to lead to an electronic delocalisation. Moreover, upon deintercalation in the Li_xCoO_2 system, each time a hole is created in the t_{2g} band, a lithium ion vacancy is formed in the lithium plane. For small deintercalation amounts, the hole remains localised in the vicinity of the lithium ion vacancy in order to ensure the electroneutrality at the local scale. Therefore, the lithium distribution tends to increase the hole localisation tendency. In the lithium-poor solid solution ($0.50 \leqslant x \leqslant 0.74$), the number of holes in the t_{2g} band, and of lithium vacancies in the lithium plane, is significantly larger, leading to a significant degree of screening which induces metallic properties. In fact, the conductivity is quite small for a metal. One can assume that the lithium/vacancy distribution, which is completely frozen at low temperature and must be fluctuating in the vicinity of room temperature, acts as scattering centres and thus lowers the mobility of electronic carriers. This general behavior of the Li_xCoO_2 phases is also to be compared with that observed for cobalt oxyhydroxides.[22] $HCoO_2$ is an insulator while the oxidised phases become semiconducting and finally metallic upon cobalt oxidation.

This set of electronic transport data indicates a rather continuous evolution of properties during deintercalation in the Li_xCoO_2 system. Therefore, this raises the following questions: why is there phase demixing and is it directly related to the changes in electronic properties? In order to try to clarify this point, a ^7Li NMR study has been performed.

^7Li MAS NMR study

Fig. 8 shows the ^7Li MAS NMR spectra of the starting $LiCoO_2$ and of the various deintercalated samples. As already reported, $LiCoO_2$ exhibits a single narrow signal very close to δ 0.[12,13] Indeed, LS Co^{III} is diamagnetic, so that no hyperfine interaction is expected for lithium in this material.

The spectra for $0.96 \leqslant x \leqslant 1.0$ all exhibit the same single signal, and are therefore not shown in Fig. 8. However, the magnitude of the signal changes with x, as shown in Fig. 9, with an expanded ppm scale, and a common absolute scale for the magnitude. The integrated signal intensity for each sample including the spinning sidebands is also given. Strict quantitativity cannot indeed be claimed for separate experiments; however, all parameters were kept as constant as possible in this series: amount of material, number of scans, probe tuning process and of course NMR parameters. Thus, an accuracy of $\pm 10\%$ is estimated for the signal magnitudes reported in Fig. 9. These values clearly show a much stronger decrease in the signal intensity than expected by considering

Table 3 Variation of the calculated critical distance R_c and of the experimental Co–Co distance with lithium amount x in Li_xCoO_2 phases

x in Li_xCoO_2	1.0	0.98	0.94[a]	0.75[a]	0.70	0.60
R_c/Å	2.900	2.898	2.895	2.880	2.878	2.868
d_{Co-Co}/Å	2.8155(2)	2.815(3)	2.813(1)	2.810(1)	2.811(1)	2.810(1)

[a]Limit of the solid solution; contains traces of the other phase.

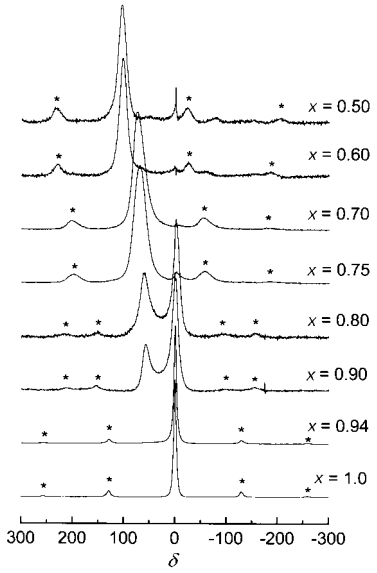

Fig. 8 ^{7}Li MAS NMR spectra for the various Li_xCoO_2 deintercalated phases (*=spinning sidebands). The δ 0 signals found for $x=0.50$ and $x=0.60$ are artifacts from the irradiation pulse.

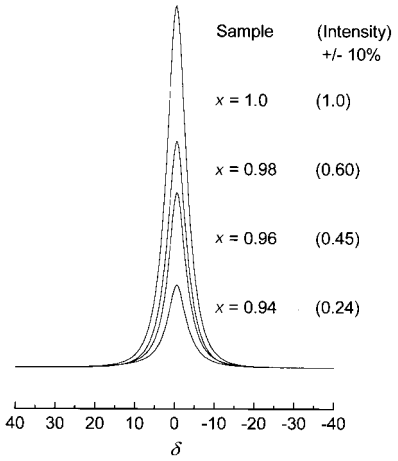

Fig. 9 ^{7}Li MAS NMR spectra for the Li_xCoO_2 samples for $0.94 \leqslant x \leqslant 1$, with an absolute intensity scale. The total integrated intensity of the signal is also given.

the small decrease in lithium concentration. Therefore, it clearly evidences a strong and gradual loss of observability for the ^{7}Li NMR signal when lithium is deintercalated in this composition range. Since some cobalt ions have necessarily been oxidised to the 4+ state, with the t_2^5 electronic configuration, one might have expected the appearance of a new signal for lithium, with a hyperfine interaction, like that due to Ni^{III} ions ($t_2^6e^1$) observed in the $Li(Ni,Co)O_2$ solid solution.[13] However, in this latter case, the transfer of the hyperfine interaction toward lithium occurs *via* the overlap with oxygen orbitals, either with a 180° (second neighbour) or a 90° geometry (first neighbour). In the present case, the single electron is present in one of the t_2 orbitals of the Co^{IV} ions, which points directly toward the 2s orbital of the neighbouring lithium ion through the common edge of the CoO_6 and LiO_6 octahedra. Therefore, one can consider that the transferred hyperfine interaction, as well as the dipolar contribution, is so strong that the ^{7}Li NMR signal is no longer observable, at least under the present experimental conditions. This clearly confirms the localised character of the single electron on Co^{IV} for $0.94 \leqslant x < 1.0$. Note that the interaction just discussed should imply the loss of observability of six Li^+ ions per Co^{IV} ion (interaction through the common edge of the octahedra). However, Fig. 9 shows that the observed loss in signal intensity is much larger. Even though the electron hole is considered to be localised in the vicinity of the lithium vacancy, a significant hopping takes place, as shown by the strong increase in the conductivity and the strong decrease in the activation energy (Fig. 5). This hopping may involve all the cobalt ions surrounding a given lithium vacancy; in addition, the lithium vacancy itself must also experience an ionic hopping within the interlayer plane. Since the NMR timescale (10^{-6} s) is considerably larger than the electronic hopping one (10^{-12} s) and comparable to the ionic hopping one, the t_{2g} single electron may interact with many Li^+ ions during the recording of the active part of the FID (*ca.* 5 ms), which leads to their not being observable in our experimental conditions.

Careful observation of the $x=0.94$ signal in Fig. 8 reveals the appearance of a weak new signal, shifted by 57 ppm. This signal grows at the expense of the δ 0 signal one when x decreases down to 0.75, that is within the two-phase region identified by X-ray diffraction. For $x<0.75$, the δ 0 signal has disappeared, and the new signal shifts further. This new signal is therefore due to the second phase, with a composition close to $Li_{0.75}CoO_2$ within the two-phase domain, and with a composition corresponding to the global one in the single-phase domain. Based on the electronic properties discussed above, it is clear that an electronic delocalisation occurs in this material. This changes the nature of the hyperfine interaction experienced by lithium from a paramagnetic contact shift type to a Knight shift one due to the participation of its orbitals to the conduction band. The delocalisation somehow spreads out the interaction over all lithium ions, instead of concerning only those in contact with localised Co^{IV} ions. This restores the observability of the ^{7}Li NMR signal and leads to a single signal for all the lithium ions in the metallic phase.

Another interesting observation is that the Knight shift observed for $x=0.5$ is very close to that for $x=0.6$. This must be due to the monoclinic distortion which occurs for x close to 0.5; indeed, this change in the crystal structure must induce changes in the band structure, so that the Knight shift no longer increases continuously with the charge carrier concentration.

Conclusion

Crystallographic and electrochemical studies have shown that our results are in complete agreement with all the previous and detailed structural studies on $LiCoO_2$.

The physical properties study has shown the presence of a few charge carriers in the starting material, which is somewhat surprising. The hypothesis of high spin Co^{3+} in the starting $LiCoO_2$, as suggested by Molenda *et al.*,[8] has to be rejected for the reasons detailed in the introduction. Therefore, the high value of the thermoelectronic power and the semiconductor character of $LiCoO_2$ can be easily explained by a small

departure from the ideal lithium stoichiometry due to the high temperature synthesis. This may lead to the presence of a few Co^{IV} ions in the starting material Co^{III} lattice.[7] This hypothesis is fully consistent with the ^7Li NMR study of the Li_xCoO_2 solid solution for $0.94 < x \leqslant 1.0$. Indeed, since localised Co^{IV} ions simply lead to the loss of observation of the neighbouring Li^+ ions, one cannot exclude that some Co^{IV} ions are already present in the starting $LiCoO_2$.

When cobalt is oxidised upon lithium deintercalation, the electronic properties as well as the ^7Li NMR study have shown the localised character of the Co^{IV} ions down to the $x = 0.94$ composition. At this point, a second phase appears with a delocalised-electron type behavior. Whereas the electronic properties vary in a smooth way, NMR clearly shows a drastic change in the electronic interactions experienced by lithium (loss of observability for Li^+ surrounding localised Co^{4+}; Knight-shifted signal for lithium belonging to the metallic phase). Moreover, NMR evidences that the metal–non-metal transition is strictly associated to the phase transition. This electronic delocalisation is therefore the driving force for the phase separation, since the two phases are otherwise crystallographically very similar. This two-phase domain could not be predicted by the first principles calculations carried out by Van der Ven *et al.*[17] within the local density approximation, so that these authors hypothesized an insulator to metal transition as its driving force. This is indeed fully confirmed by our investigations, in particular thanks to the very strong sensitivity of NMR to the hyperfine interactions with paramagnetic or delocalised electrons. This property was indeed pointed out by Berthier *et al.*[23] in a conductivity and NMR study of the Li_xZrSe_2 system, where they also evidenced a non-metal–metal transition upon intercalation. In that case, the ^{77}Se NMR shift was constant in the semiconducting region for $x \leqslant 0.4$, whereas the Knight shift increased with x in the metallic region ($x > 0.4$). However, the ^7Li NMR shift was reported to be only very slightly different in the two regions, which indicates a much smaller participation of the Li 2s orbital to the conduction band than in the case of Li_xCoO_2.

Just before submission of the present paper, Imanishi *et al.*[24] presented ^7Li MAS NMR and conductivity results on deintercalated Li_xCoO_2 samples, which are in very good agreement with ours. However, the loss of observability of the NMR signal in the localised Co^{IV} region was not mentioned.

Acknowledgements

The authors wish to thank J. P. Doumerc for fruitful discussions, E. Marquestaut for technical assistance and Région Aquitaine for financial support.

References

1 K. Mizushima, P. C. Jones, P. J. Wiseman and J. B. Goodenough, *Mater. Res. Bull.*, 1980, **15**, 783.
2 J. N. Reimers and J. R. Dahn, *J. Electrochem. Soc.*, 1992, **139**, 2091.
3 T. Ohzuku and A. Ueda, *J. Electrochem. Soc.*, 1994, **141**, 2972.
4 G. G. Amatucci, J. M. Tarascon and L. C. Klein, *J. Electrochem. Soc.*, 1996, **143**, 1114.
5 M. Shibuya, T. Nishina, T. Matsue and I. Uchida, *J. Electrochem. Soc.*, 1996, **143**, 3157.
6 M. Nishizawa, S. Yamamura, T. Itoh and I. Uchida, *Chem. Commun.*, 1998, 1631.
7 A. Honders, J. M. der Kinderen, A. H. Van Heeren, J. H. W. de Witt and G. H. J. Broers, *Solid State Ionics*, 1984, **14**, 205.
8 J. Molenda, A. Stoklosa and T. Bak, *Solid State Ionics*, 1989, **36**, 53.
9 I. Saadoune and C. Delmas, *J. Solid State Chem.*, 1998, **136**, 8.
10 C. Delmas, J. J. Braconnier, Y. Borthomieu and P. Hagenmuller, *Mater. Res. Bull.*, 1987, **22**, 741.
11 H. J. Orman and P. J. Wiseman, *Acta Crystallogr., Sect. C*, 1984, **40**, 12.
12 M. Ménétrier, A. Rougier and C. Delmas, *Solid State Commun.*, 1994, **90**, 439.
13 C. Marichal, J. Hirschinger, P. Granger, M. Ménétrier, A. Rougier and C. Delmas, *Inorg. Chem.*, 1995, **34**, 1773.
14 I. Saadoune, M. Ménétrier and C. Delmas, *J. Mater. Chem.*, 1997, **7**, 2505.
15 B. Ouyang, X. Cao, H. W. Lin, S. Slane, S. Kostov, M. d. Boer and S. G. Greenbaum, *Mater. Res. Soc. Symp. Proc.*, 1995, **369**, 59.
16 M. Ménétrier, I. Saadoune, S. Levasseur and C. Delmas, *Extended Abstract of the 9th International Meeting on Lithium Batteries*, Edinburgh, 12–17 July 1998, Poster II, Thur 16.
17 A. Van der Ven, M. K. Aydinol, G. Ceder, G. Kresse and J. Hafner, *Phys. Rev. B*, 1998, **58**, 2975.
18 P. Dordor, E. Marquestaut and G. Villeneuve, *Rev. Phys. Appl.,* 1980, **15**, 1607.
19 W. Li, J. N. Reimers and J. R. Dahn, *Solid State Ionics*, 1993, **67**, 123.
20 H. Arai, S. Okada, H. Ohtsuka, M. Ichimura and J. Yamaki, *Solid State Ionics*, 1995, **80**, 261.
21 J. B. Goodenough, *Prog. Solid State Chem.*, 1971, **5**, 278.
22 M. Butel, L. Gautier and C. Delmas, *Solid State Ionics*, in press.
23 C. Berthier, Y. Chabre, P. Ségransan, P. Chevalier, L. Trichet and A. Le Mehauté, *Solid State Ionics*, 1981, **5**, 379.
24 N. Imanishi, M. Fujiyoshi, Y. Takeda and O. Yamamoto, *Extended Abstract of the 39th Battery Symposium in Japan*, Sendaï, 25–27 November 1998, p. 303.

Paper 9/00016J